

## VHE $\gamma$ -ray/X-ray correlation studies in Mrk 421 down to the quiescent state

---

### **Barbara Patricelli\***

*Università di Pisa, INFN - Sezione di Pisa, Instituto de Astronomía - UNAM*

*E-mail: [barbara.patricelli@pi.infn.it](mailto:barbara.patricelli@pi.infn.it)*

### **Magdalena González**

*Instituto de Astronomía - UNAM*

*E-mail: [magda@astro.unam.mx](mailto:magda@astro.unam.mx)*

### **Nissim Fraija**

*Instituto de Astronomía - UNAM*

*E-mail: [nifraija@astro.unam.mx](mailto:nifraija@astro.unam.mx)*

The blazar Mrk 421 is one of the closest, brightest and fastest varying source in the extragalactic X-ray/TeV sky. In the last years, many multi-wavelength campaigns have been carried out to study the correlation between the very high energy (VHE)  $\gamma$ -ray and X-ray fluxes of this source and, although the activity in these two energy ranges seems to be correlated in many observations, no conclusive results have been achieved yet. In this work we present a robust study of the VHE  $\gamma$ -ray/X-ray correlation of Mrk 421 with data taken with different VHE experiments on different time scales and for different levels of activity of the source, with special focus on the low activity states. In particular, we discuss the robustness of the correlation at the lowest fluxes corresponding to the quiescent state of Mrk 421.

*The 34th International Cosmic Ray Conference,  
30 July- 6 August, 2015  
The Hague, The Netherlands*

---

\*Speaker.

## 1. Introduction

Blazars are active galactic nuclei (AGN) with relativistic jets closely aligned to our line of sight. They show intense flux variability on different time scales and at all wavelengths. Their broadband spectral energy distribution (SED) shows a double-peaked structure, with a “hump” at low energies, peaking in radio through X-rays and a second “hump” at higher energies, peaking in  $\gamma$ -rays. While there is ample evidence that the low energy peak is due to synchrotron radiation from the relativistic electrons within the jet, there are two competing scenarios to explain the high energy peak: the so-called leptonic models (e.g. synchrotron self-Compton, SSC or external Compton, EC) and the hadronic models. To put some constraints on the proposed theoretical models, simultaneous multiwavelength observations of these sources over long periods of times are needed. For instance, a useful tool to discriminate between the models is the study of the correlation between VHE  $\gamma$ -rays and X-rays, since such a correlation is expected in the SSC scenario, while it is difficult to be explained within hadronic models (see, however, [1, 2]).

In the last years, several studies have been performed to investigate the VHE  $\gamma$ -ray/X-ray correlation in different blazars. Positive heterogeneous correlations between the VHE  $\gamma$ -ray and the X-ray emission have been reported during flaring activity of several blazars (see, e.g., [3, 4]), although there are also cases in which the correlation is fairly loose (see, e.g. [5]), or even “orphan TeV flares”, i.e. VHE  $\gamma$ -ray flares without X-ray activity have been reported (see [6]). Positive correlations have been found also when considering long term observation periods covering different levels of activity of the source, from the low state to the highest states. For instance, Acciari et al. 2014 [7] reported on a 14-year monitoring of the blazar Mrk 421 and they showed that a correlation between the X-ray and TeV energy bands is present, although the found correlation presents a considerable scatter.

The low state has been poorly studied at VHE, mainly due to the limited sensitivity of the current VHE  $\gamma$ -ray observatories and because the VHE  $\gamma$ -ray observations are usually only triggered when the source is in a high state of activity at other wavelengths. There are, however, a few studies pointing out the presence of a correlation also for the quiescent state of blazars. For instance, Aleksić et al. 2015 [8] recently reported on a positive correlation between the VHE  $\gamma$ -ray and X-ray emission of the blazar Mrk 421 during a low state of activity, and suggested that the physical processes dominating the emission during non-flaring states have similarities with those occurring during flaring activity for this source.

A direct comparison of all these results would be useful to better investigate the possible differences among flares and between the flaring and the quiescent state of blazars, as well as to study if the correlation depends on the time scale; however, this is a difficult task because data from different experiments are reported in an heterogeneous way (i.e., for VHE  $\gamma$ -ray data different energy thresholds and units are used).

Here we combine together several sets of simultaneous VHE  $\gamma$ -ray and X-ray observations taken by different experiments, on different time scales and for different monitoring periods for the blazar Mrk 421. We convert all the data to the same energy threshold/range and units, to make them directly comparable and present a study of the correlation between the X-ray and the VHE  $\gamma$ -ray emission. In particular, our analysis is focused on the lower fluxes characterizing the quiescent state of Mrk 421.

## 43 2. The data sets

44 The most unbiased and comprehensive data set of simultaneous VHE  $\gamma$ -ray/X-ray observations  
 45 of Mrk 421 is the one presented by Acciari et al. 2014 [7], that reported on a long term (14-year)  
 46 monitoring of Mrk 421 with the Whipple 10 m telescope. They combined the Whipple data with  
 47 simultaneous RXTE/ASM data and found that the VHE  $\gamma$ -ray fluxes are linearly correlated with  
 48 the X-ray fluxes on monthly time-scale, although the present large scatter was not quantified. To  
 49 investigate the possible dependence of the correlation from the time scale and from the experiment  
 50 by which data have been taken, we combine the Whipple-RXTE/ASM data with other published  
 51 data sets that allow a good flux sampling over a large range of flux values (from the quiescent state  
 52 flux up to the most intense flare fluxes) and over different time scales. We then apply a statistical  
 53 approach that allow us to estimate if all the data are correlated, the robustness of the correlation and  
 54 how significant are the deviations from it. In the following we briefly summarize the characteristics  
 55 of the additional data sets we used.

56 *The HEGRA CT1-RXTE/ASM data.* - Aharonian et al. 2003 [9] reported on the monitoring  
 57 of Mrk 421 with HEGRA CT1 during a period of intense activity of the source in 2001. They  
 58 combined the HEGRA CT1 data with simultaneous RXTE/ASM data and found that the VHE  
 59  $\gamma$ -ray fluxes are linearly correlated with the X-ray fluxes on hourly time scale.

60 *The MAGIC/Whipple/VERITAS-XMM Newton data.* - Acciari et al. 2009 [10] reported on the  
 61 monitoring of Mrk 421 during two flaring states: one on April 2006, with VHE  $\gamma$ -ray data from  
 62 MAGIC and Whipple and, the other on May 2008 with data from VERITAS. They combined the  
 63 VHE  $\gamma$ -ray data with simultaneous XMM-Newton data, in the energy range of 0.5-10 keV (similar  
 64 to RXTE/ASM data) and pointed out the lack of correlation on a time scale of  $\sim 20$ -30 minutes  
 65 during the first flare.

66 *The MAGIC-RXTE/ASM data.* - Albert et al. 2007 [11] reported on the monitoring of Mrk  
 67 421 from November 2004 to April 2005 with MAGIC. They combined the MAGIC data with  
 68 simultaneous RXTE/ASM data and found that the VHE  $\gamma$ -ray fluxes are correlated with the X-ray  
 69 fluxes on a nightly time scale.

70 To compare all these data sets, the measured VHE  $\gamma$ -ray and X-ray fluxes must be converted  
 71 to a common energy threshold (or energy range) and be expressed in the same units. For the VHE  
 72  $\gamma$ -ray data we choose an energy threshold of 400 GeV and the Crab units, while for the X-ray data  
 73 an energy range (2-10 keV) and the units of RXTE/ASM counts/s, the same reported in [7].

74 To convert the VHE  $\gamma$ -ray fluxes from an energy threshold  $E_0$  to the new energy threshold  $E_1$   
 75 (400 GeV) in Crab units we use the following relation:

$$F(E > E_1) = F(E > E_0) \times \frac{\int_{E_1}^{\infty} \phi(E) dE}{\int_{E_0}^{\infty} \phi(E) dE \times \int_{E_1}^{\infty} \phi_{\text{Crab}}(E) dE}, \quad (2.1)$$

76 where  $\phi(E)$  and  $\phi_{\text{Crab}}(E)$  are the source and the Crab spectrum respectively. To do this conversion,  
 77 we take the spectra observed by the corresponding instrument and when possible for the same time  
 78 period of the corresponding observation to minimize discrepancies between different data sets due  
 79 to systematic effects of the experiment [9, 10, 11, 12, 13, 14, 15].

80 To convert the X-ray fluxes in RXTE/ASM rates we use the online WebPIMMS<sup>1</sup> tool.

<sup>1</sup><http://heasarc.gsfc.nasa.gov/cgi-bin/Tools/w3pimms/w3pimms.pl>

### 81 3. The VHE $\gamma$ -ray/X-ray correlation

82 We study the VHE  $\gamma$ -ray/X-ray correlation for Mrk 421 using all the data sets described in the  
83 previous section, with all the fluxes converted to the chosen units and energy threshold/range.

84 The VHE  $\gamma$ -ray and X-ray fluxes are linearly correlated, with a Pearson correlation coefficient  
85  $R = 0.81$ . To estimate how robust is the correlation we use the maximum likelihood approach  
86 described in [16]. This method assumes that, if the correlated data (in our case the X-ray and  
87 VHE  $\gamma$ -ray fluxes  $F_{x,i}$  and  $F_{\gamma,i}$ ) can be described by a linear function  $F_{\gamma} = aF_x + b$  with an intrinsic  
88 scatter  $\sigma$ , the optimal values of the parameters ( $a$ ,  $b$  and  $\sigma$ ) can be determined by minimizing the  
89 minus-log-likelihood function:

$$L(a, b, \sigma) = \frac{1}{2} \sum_i \log(\sigma^2 + \sigma_{F_{\gamma,i}}^2 + a^2 \sigma_{F_{x,i}}^2) + \frac{1}{2} \sum_i \frac{(F_{\gamma,i} - aF_{x,i} - b)^2}{\sigma^2 + \sigma_{F_{\gamma,i}}^2 + a^2 \sigma_{F_{x,i}}^2}, \quad (3.1)$$

90 where  $\sigma_{F_{x,i}}$  and  $\sigma_{F_{\gamma,i}}$  are the uncertainties on  $F_{x,i}$  and  $F_{\gamma,i}$  respectively.

91 With this method we obtain  $a = 0.66 \pm 0.04$ ,  $b = -0.01 \pm 0.05$  and  $\sigma = 0.37 \pm 0.03$ . The  
92 results are shown in the left panel of Fig. 1. It can be seen that almost all the data are positively  
93 correlated within  $3\sigma$ , therefore the correlation is robust and consistent between instruments. Such  
94 a correlation is naturally expected within the SSC scenario. However, there are intense VHE  $\gamma$ -ray  
95 fluxes that seem not to be accompanied by intense X-ray fluxes, lying at more than  $3\sigma$  above the  
96 best linear fit. It is interesting to note that these fluxes are all higher than the “high state” flux<sup>2</sup> of  
97 Mrk 421 (corresponding to 3 Crab) as measured by VERITAS [17]. Another interesting point is  
98 that the dispersion around the best fit straight line is smaller in the region of low VHE  $\gamma$ -ray fluxes,  
99 where the majority of the points lie within 1-2  $\sigma$ . This is an unexpected result: in fact, due to the  
100 limited sensitivity of the detectors, lower fluxes are expected to have larger uncertainties and larger  
101 dispersion.

102 To better study this last aspect, we repeat the whole procedure only for the quiescent state of  
103 Mrk 421. From all the data sets we select the points with a VHE  $\gamma$ -ray flux up to the VERITAS  
104 “very low” state flux of Mrk 421 [17], corresponding to 0.76 Crab<sup>3</sup> for an energy threshold of 400  
105 GeV. This value is comparable with the upper limit on the quiescent flux of Mrk 421 reported by  
106 Tluczykont et al. 2010 [18] (0.33 Crab for an energy threshold of 1 TeV, corresponding to  $\approx 0.73$   
107 Crab above 400 GeV<sup>4</sup>): this means that the observed fluxes below the VERITAS “very low” state  
108 are dominated by the emission of the source in the quiescent state.

109 These data are linearly correlated, with  $R = 0.61$ . By fitting them with the maximum likelihood  
110 approach we obtain  $a = 0.23 \pm 0.03$ ,  $b = 0.23 \pm 0.03$  and  $\sigma = 0.13 \pm 0.01$ . The results are shown  
111 in the right panel of Fig. 1. It can be seen that all the data lie within  $3\sigma$  from the best fit straight  
112 line. Therefore, also when considering the quiescent state independently, the correlation is robust,  
113 consistently with the results found by Aleksić et al. 2015 [8]: this suggests that SSC dominates the

<sup>2</sup>We refer as the VERITAS “high” state flux the value corresponding to the “high state A” reported in Acciari et al. 2011 [17].

<sup>3</sup>To convert the VERITAS fluxes in Crab units, we assume the VERITAS spectrum of the Crab as reported by Holder et al. 2006 [13].

<sup>4</sup>For the conversion to the energy threshold of 400 GeV we assume the VERITAS spectra for the Crab and Mrk 421 [13, 17].

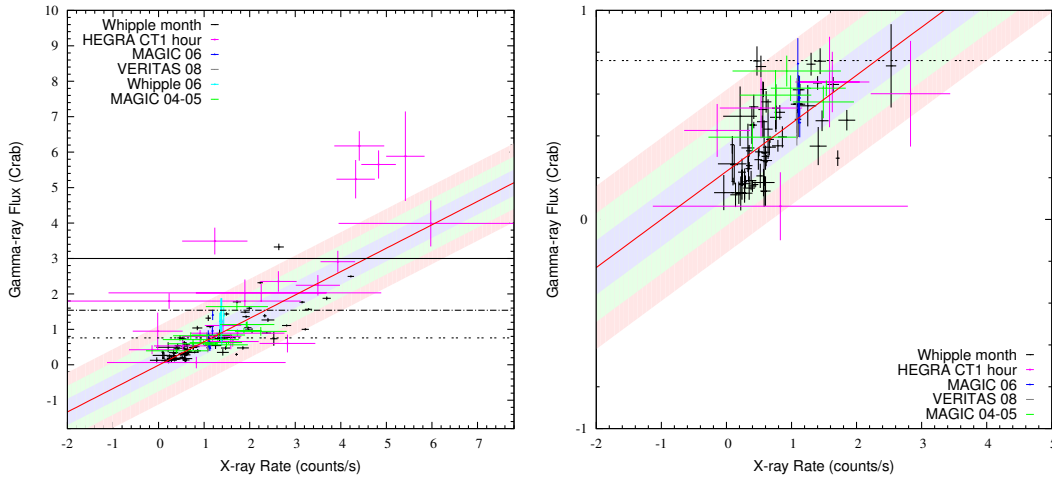


**Figure 1:** Left panel: correlation between the X-ray (2-10 keV) and the VHE  $\gamma$ -ray ( $E > 400$  GeV, Crab) fluxes of Mrk 421 with data from different X-ray satellites and VHE  $\gamma$ -ray experiments (see text). The red solid line is the best fitting straight line. The shadowed regions represent the 1, 2 and 3  $\sigma$  scatter around the best fit of this correlation; for comparison, the “very low”, “low” and “high” state flux levels of Mrk 421, as measured by VERITAS [17] are shown as black dotted, dot-dashed and solid lines respectively. Right panel: same as left panel, but the fit has been done considering only data with VHE  $\gamma$ -ray fluxes up to 0.76 Crab, corresponding to the VERITAS “very low” state flux of Mrk 421 [17].

114 emission of Mrk 421 not only during flares, but also during the quiescent state. It is interesting to  
 115 note that the intrinsic scatter of the correlation for the quiescent state is about a factor of 3 smaller  
 116 that the one obtained for the overall correlation.

117 The correlation for the quiescent state and the one obtained fitting together all the data are  
 118 consistent, within 3  $\sigma$ , up to X-ray fluxes of  $\sim 4$  counts/s.

#### 119 4. Conclusions

120 We presented a study of the VHE  $\gamma$ -ray/X-ray correlation for the blazar Mrk 421. We used  
 121 several data collected by different VHE  $\gamma$ -ray experiments and X-ray satellites on different time  
 122 scales and for different monitoring periods of the source. We converted all the fluxes in the same  
 123 units and with the same energy threshold/range, in order to make them directly comparable and we  
 124 performed a statistical study of the overall correlation, as well as of the correlation for the quiescent  
 125 state of the source. We found that in both cases data are linearly correlated and that the correlations  
 126 are robust and consistent within instruments, suggesting SSC as the dominating emission process.  
 127 We also found that the two correlations are consistent between themselves within 3  $\sigma$ , and that  
 128 the dispersion of the data around the best fit straight line is smaller for the quiescent state. A  
 129 more detailed analysis of the results here presented and of their theoretical interpretation will be  
 130 presented elsewhere.

131 **Acknowledgments**

132 This work was supported by Luc Binette scholarship and DGAPA-UNAM under PAPIIT  
133 project IG100414-3.

134 **References**

- 135 [1] Mücke, A., et al., *BL Lac objects in the synchrotron proton blazar model*, *Astroparticle Physics* **18**  
136 (2003) 593
- 137 [2] Mastichiadis, A., et al., *Mrk 421 as a case study for TeV and X-ray variability in leptohadronic*  
138 *models*, *MNRAS* **434** (2013) 2684
- 139 [3] Fossati, G., et al., *Multiwavelength Observations of Markarian 421 in 2001 March: An Unprecedented*  
140 *View on the X-Ray/TeV Correlated Variability*, *ApJ* **677** (2008) 906
- 141 [4] Gliozzi, M., et al., *Long-Term X-Ray and TeV Variability of Mrk 501*. *ApJ* **646** (2006) 61
- 142 [5] Rebillot, P. F., et al., *Multiwavelength Observations of the Blazar Markarian 421 in 2002 December*  
143 *and 2003 January*, *ApJ* **641** (2006) 740
- 144 [6] Błażejowski, M., et al., *A Multiwavelength View of the TeV Blazar Markarian 421: Correlated*  
145 *Variability, Flaring, and Spectral Evolution*, *ApJ* **630** (2005) 130
- 146 [7] Acciari, V. A., et al., *Observation of Markarian 421 in TeV gamma rays over a 14-year time span*,  
147 *Astroparticle Physics* **54** (2014) 1
- 148 [8] Aleksić, J., et al., *The 2009 multiwavelength campaign on Mrk 421: Variability and correlation*  
149 *studies*, *A&A* **576** (2015) 126
- 150 [9] Aharonian, F., et al., *TeV gamma -ray light curve and energy spectrum of Mkn 421 during its 2001*  
151 *flare as measured with HEGRA CT1*, *A&A* **410** (2003) 813
- 152 [10] Acciari, V. A., et al., *Simultaneous Multiwavelength Observations of Markarian 421 During Outburst*,  
153 *ApJ* **703** (2009) 169
- 154 [11] Albert, J., et al., *Observations of Markarian 421 with the MAGIC Telescope*, *ApJ* **663** (2007) 125
- 155 [12] Aharonian, F., et al., *The Crab Nebula and Pulsar between 500 GeV and 80 TeV: Observations with*  
156 *the HEGRA Stereoscopic Air Cerenkov Telescopes*, *ApJ* **614** (2004) 125
- 157 [13] Holder, J., et al., *The first VERITAS telescope*, *Aph* **25** (2006) 391
- 158 [14] Grube, J., *Observations of the Crab Nebula with the Whipple 10 m Telescope*, in proceedings of  
159 *International Cosmic Ray Conference 2* (2008) 691
- 160 [15] Albert, J., et al., *VHE  $\gamma$ -Ray Observation of the Crab Nebula and its Pulsar with the MAGIC*  
161 *Telescope*, *ApJ* **674** (2008) 1037
- 162 [16] D'Agostini, G., *Fits, and especially linear fits, with errors on both axes, extra variance of the data*  
163 *points and other complications*, physics.data-an/0511182
- 164 [17] Acciari, V. A., et al., *TeV and Multi-wavelength Observations of Mrk 421 in 2006-2008*, *ApJ* **738**  
165 (2011) 25
- 166 [18] Tluczykont, M., et al., *Long-term lightcurves from combined unified very high energy gamma-ray*  
167 *data*, *A&A* **524** (2010) 48